Supplement of The Cryosphere, 20, 1405–1425, 2026
https://doi.org/10.5194/tc-20-1405-2026-supplement

The Cryosphere Open Access EGU

Supplement of

The effect of the present-day imbalance on schematic and climate forced simulations of the West Antarctic Ice Sheet collapse

Tim van den Akker et al.

Correspondence to: Tim van den Akker (tim.vandenakker@geo.su.se)

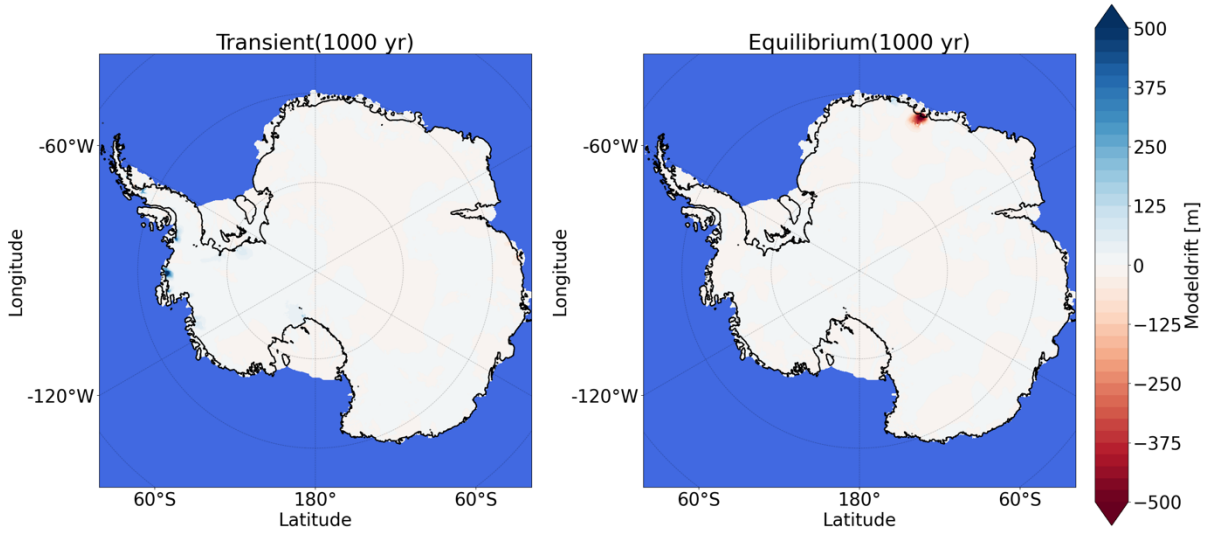

Figure S1. Ice thickness changes due to modeldrift after 1000 years of unforced simulations. The transient initalization is shown on the left, the equilibrium initialization on the right.

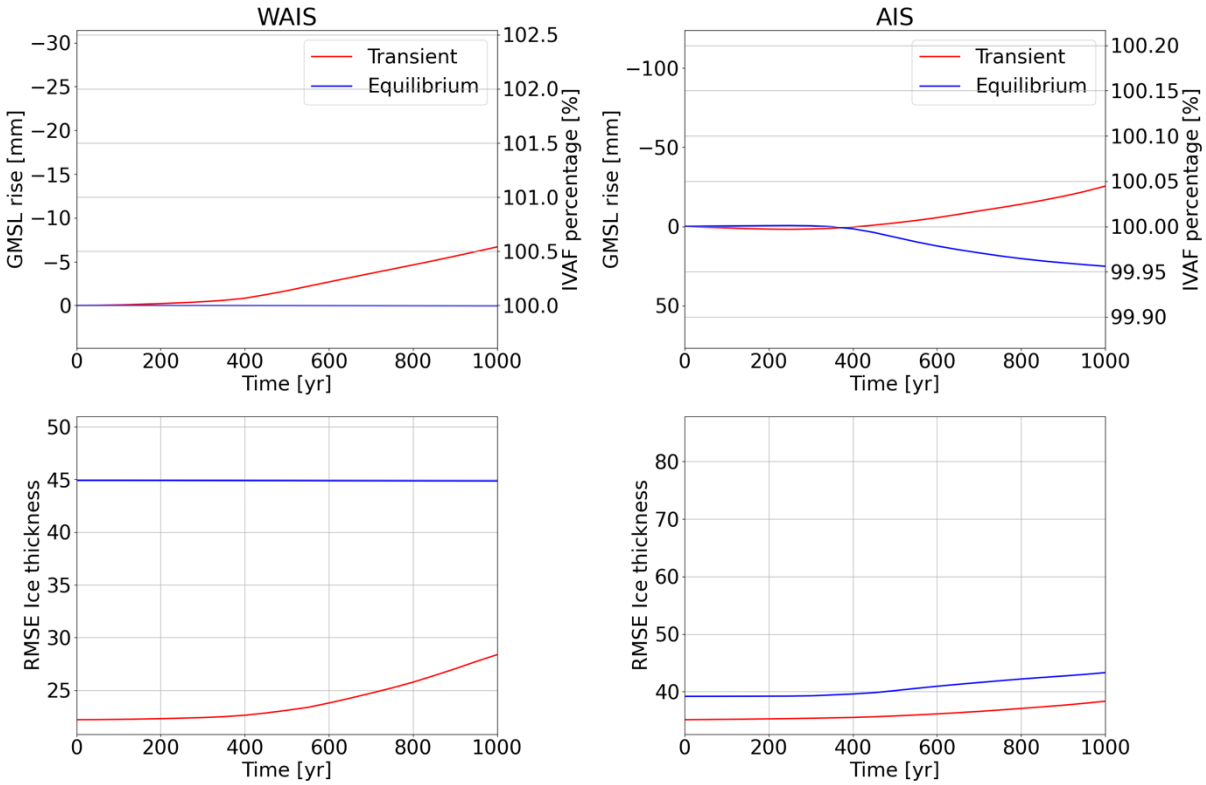

Figure S2. Modeldrift expressed as function of (upper panels) integrated GMSL rise and change in IVAF percentage and (lower panels) RMSE of modelled ice thickness wrt observations for both initializations after 1000 years of unforced simulations. The transient initalizations is shown in red, the equilibrium initialization in blue.

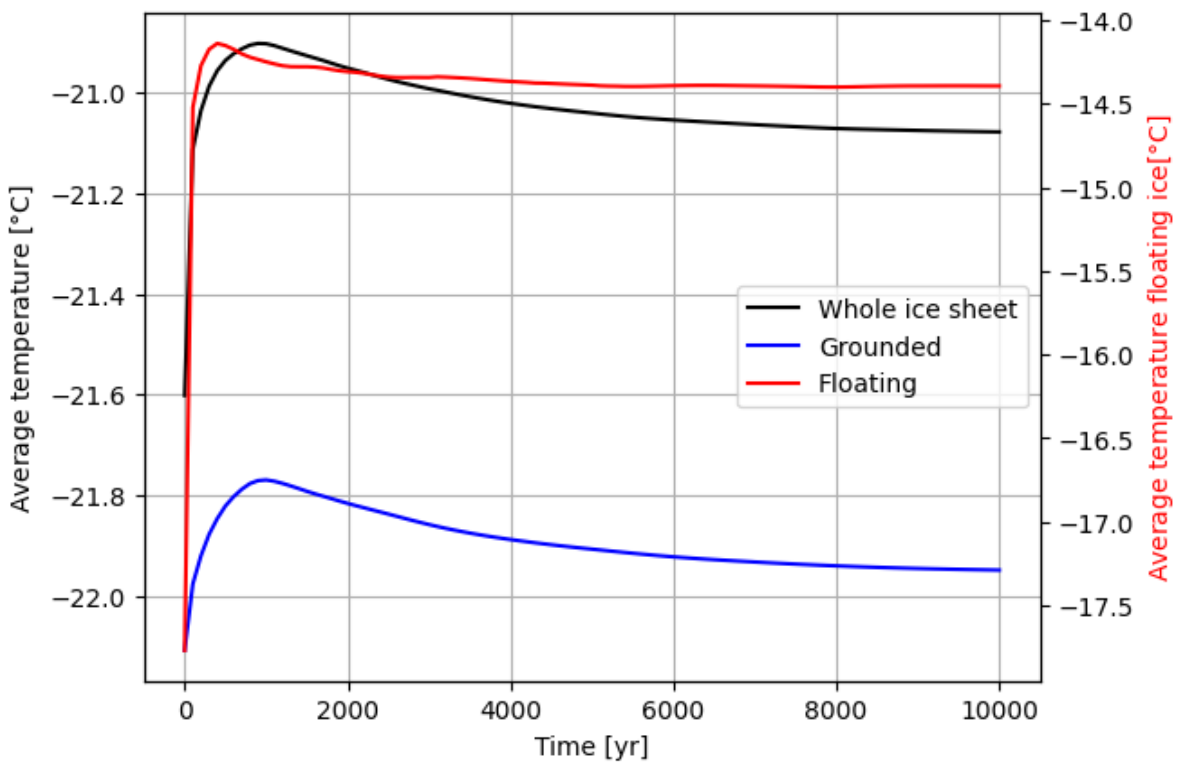

Figure S3. Grid point average temperature during the transient initialition (similar for the equilibrium initialization, not shown) for floating ice (red line, right y-axis), grounded ice (blue line, left y-axis) and all grid point containing ice (black line, right y-axis)

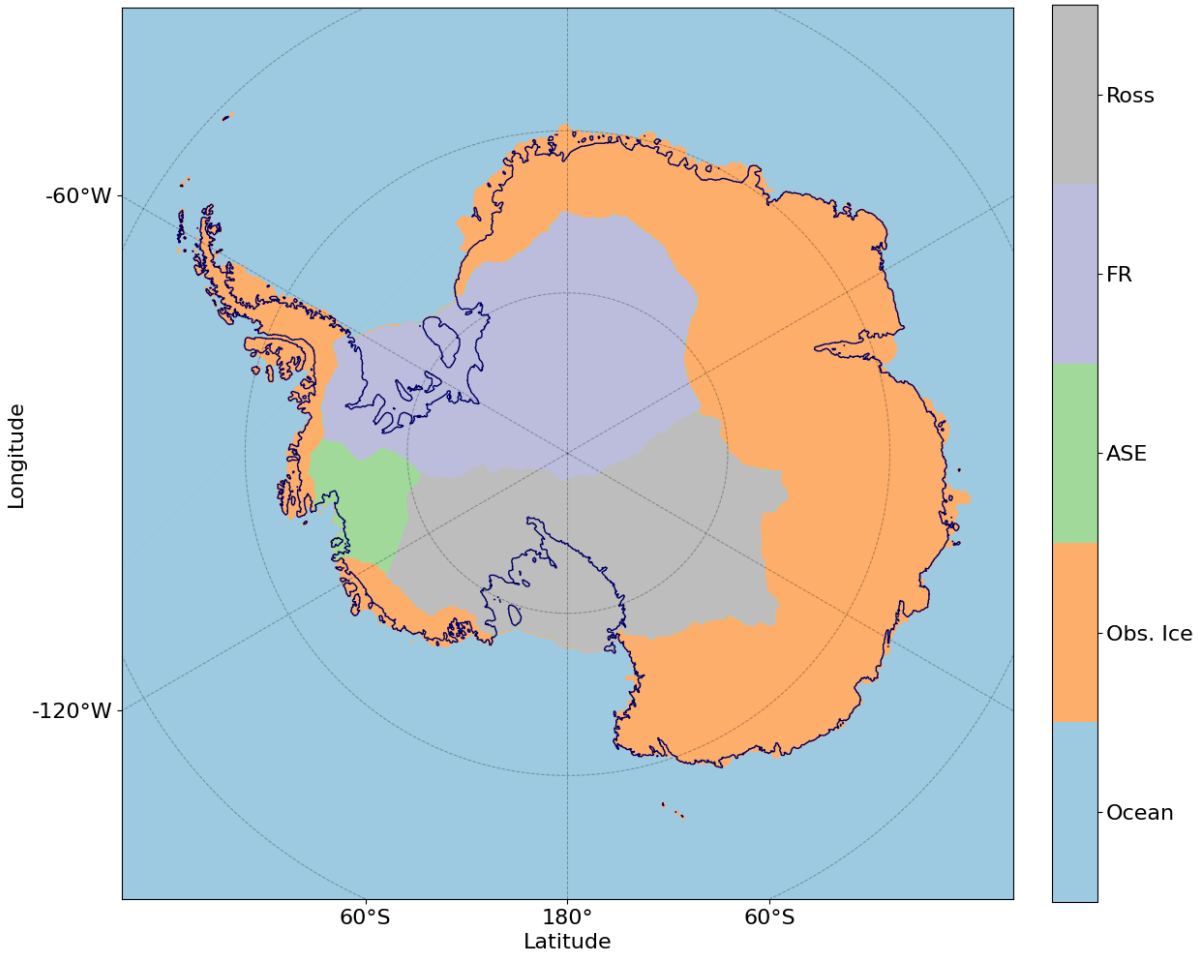

Figure S4. Regions considered in detail in this study, following the basins of Zwally et al. (2015). Observed grounding line is shown in red, the ASE basins in green, the Filchner-Ronne basins in purple and the Ross basins in grey. Grid cells with ice thickness observations are shown in orange.

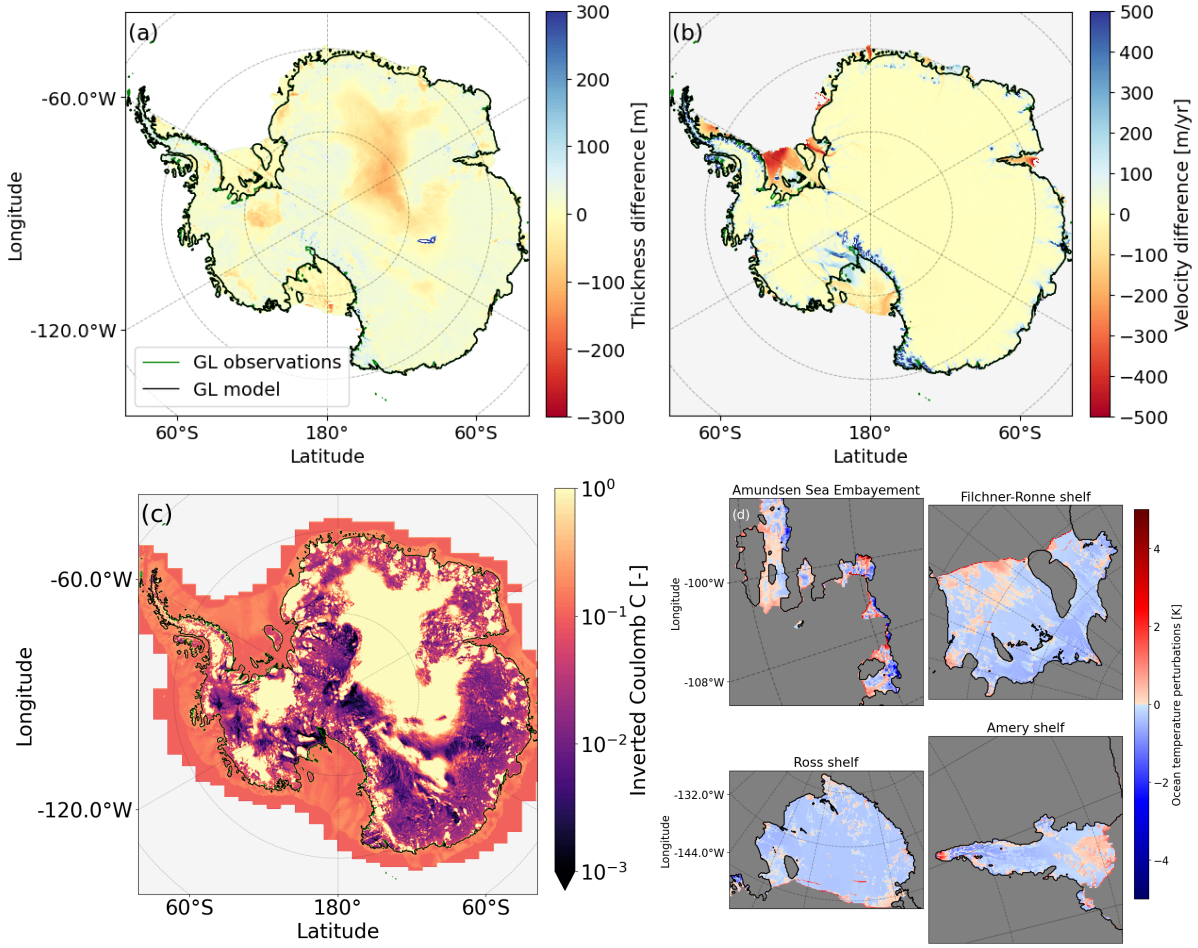

Figure S5. Modelled Antarctic Ice Sheet initialized state with the transient initialization. (a) thickness difference with respect to observations(Morlighem et al., 2020). The modelled grounding line is shown in black, and the observed grounding line in green (only visible where it does not overlap with the modelled one). (b) ice surface velocity difference with respect to the observations(Rignot et al., 2011). Positive values indicate regions where CISM overestimates the ice velocities. (c) the inverted C_c and (d) the inverted ocean temperature perturbation under the main shelves.

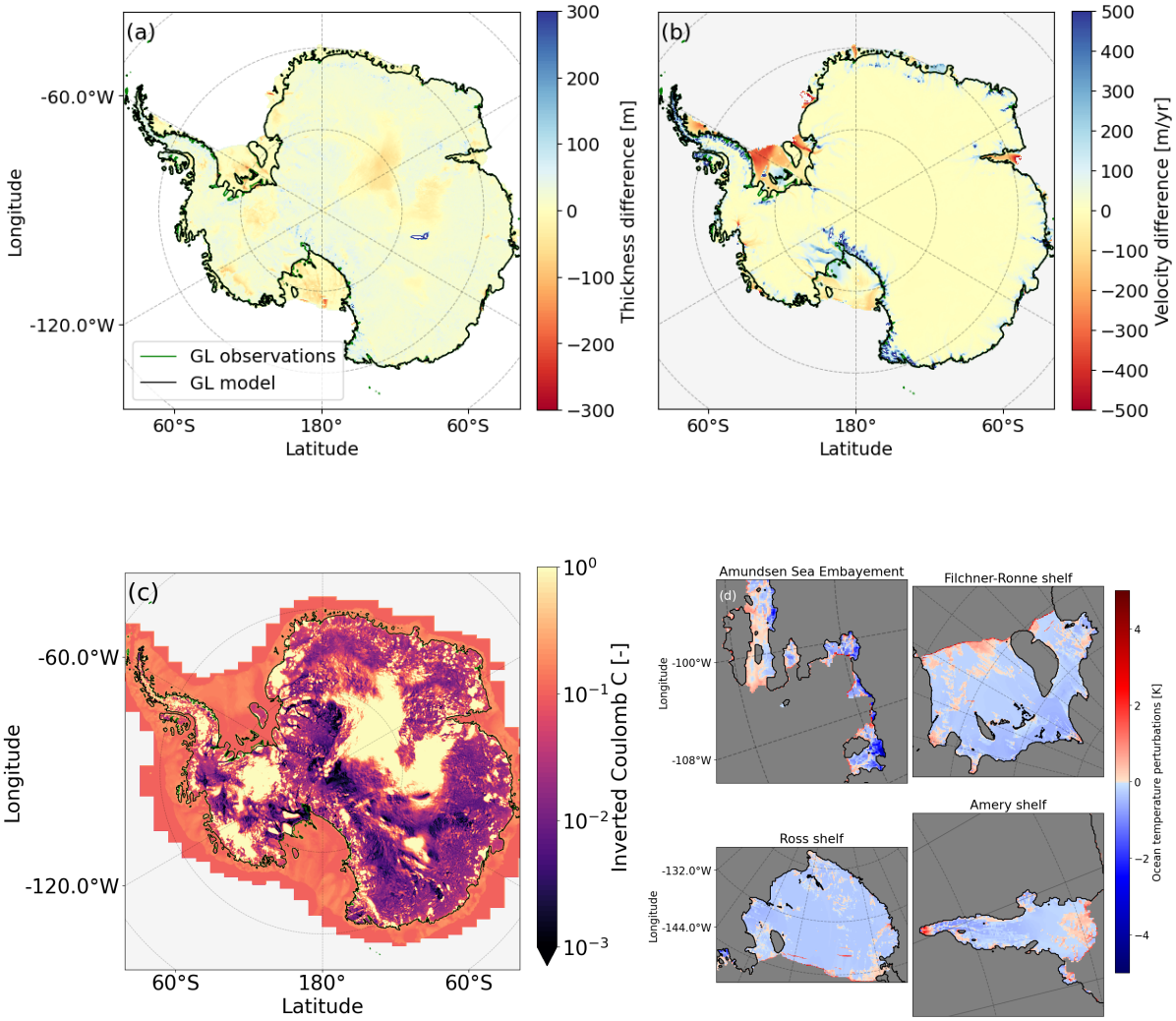

Figure S6. As in Figure S5 but for the equilibrium initialization

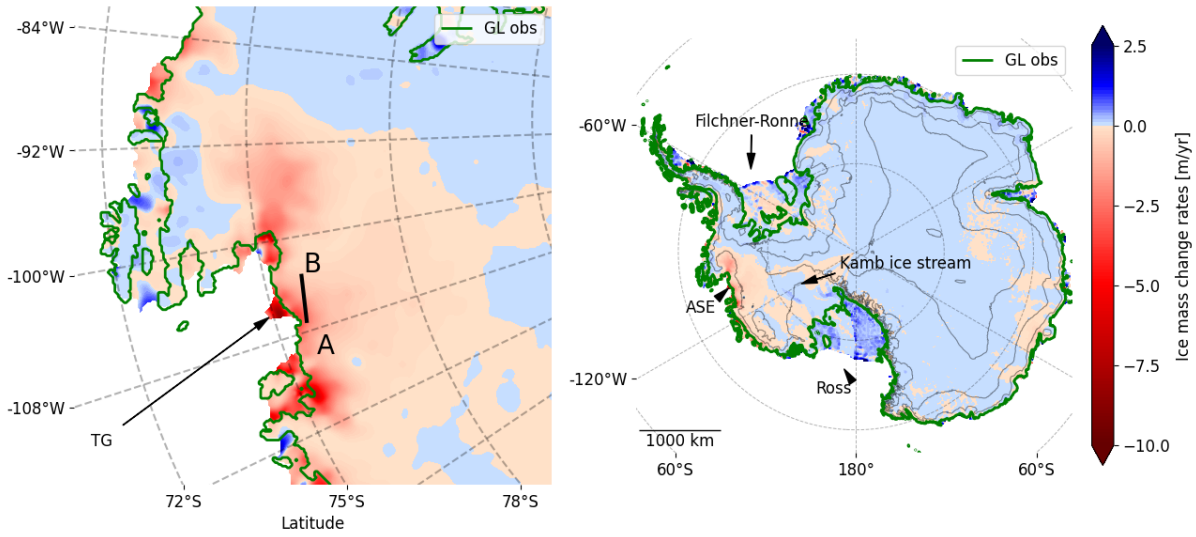

Figure S7. Mass change rates from Smith et al. (2020) interpolated to the CISM domain.

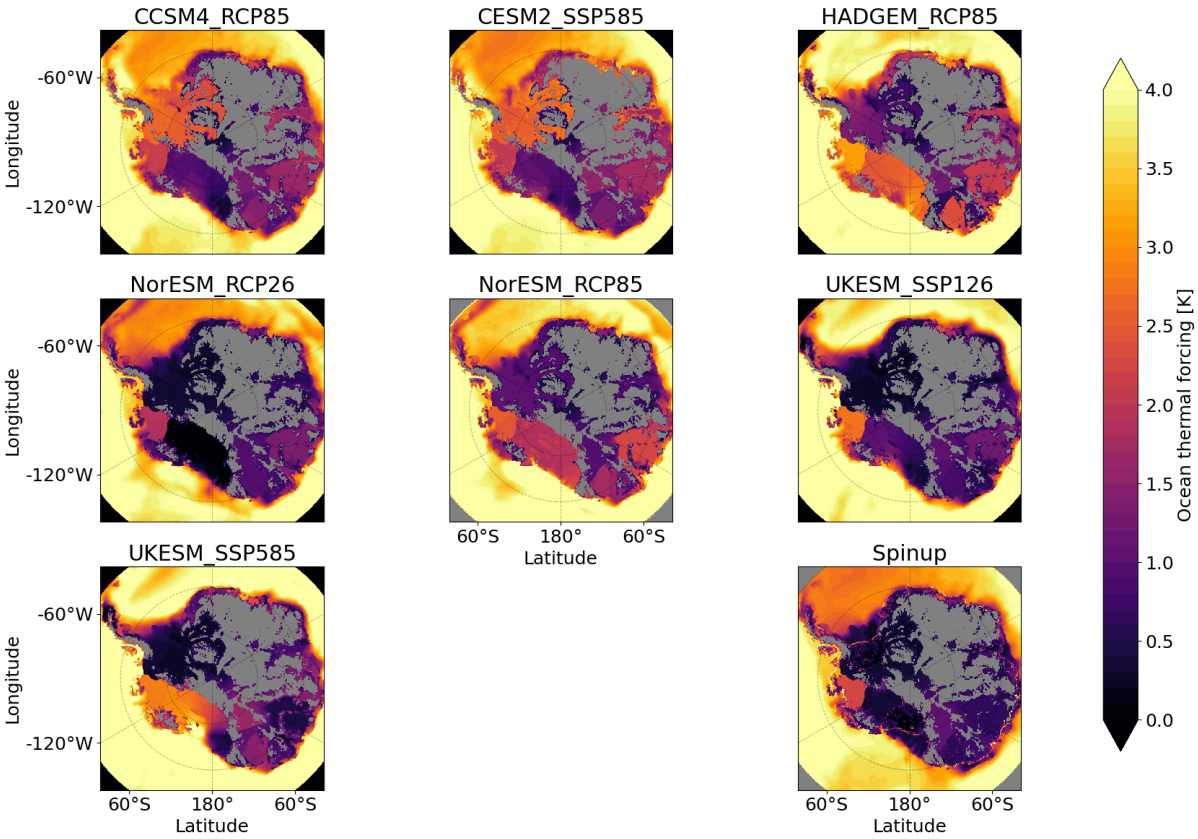

Figure S8. Thermal forcing ($TF_{\mathbf{base}} + \delta T$ in Eq. (1.5)) from the five ESMs used. Thermal forcing averages for the years 2080 – 2100 (except the spinup) are shown for a depth of -500 metres. Cells with bedrock above sea level are shown in grey.

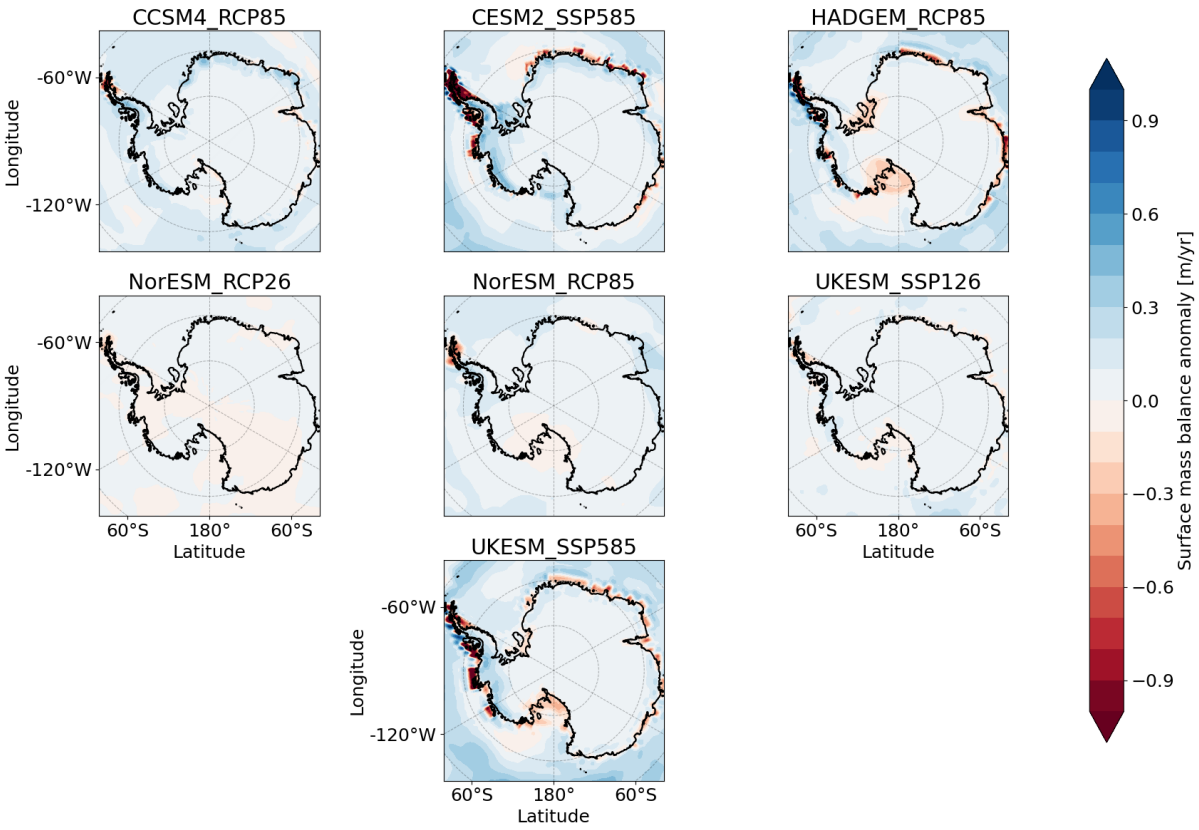

Figure S9. Surface mass balance (SMB) anomalies simulated by the five ESMs. The average of the years 2080 – 2100 is shown. Anomalies are added directly to the modelled SMB annually in the continuation simulations. The observed grounding line position is shown in black.

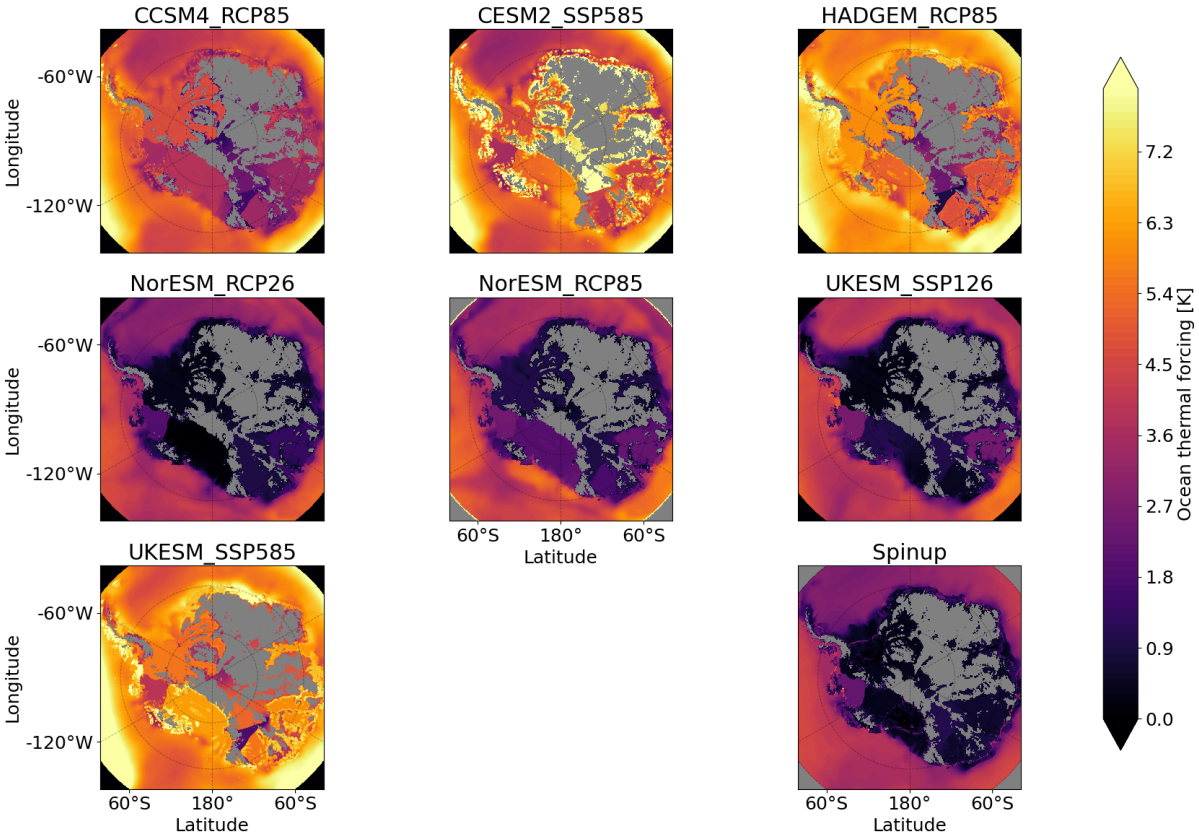

Figure S10. Thermal forcing ($TF_{\text{base}} + \delta T$ in Eq. (1.6)) from the five ESMs used. Thermal forcing averages for the years 2080 - 2300 (except the present-day) are shown for a depth of -500 metres. Cells with bedrock above sea level are shown in grey.

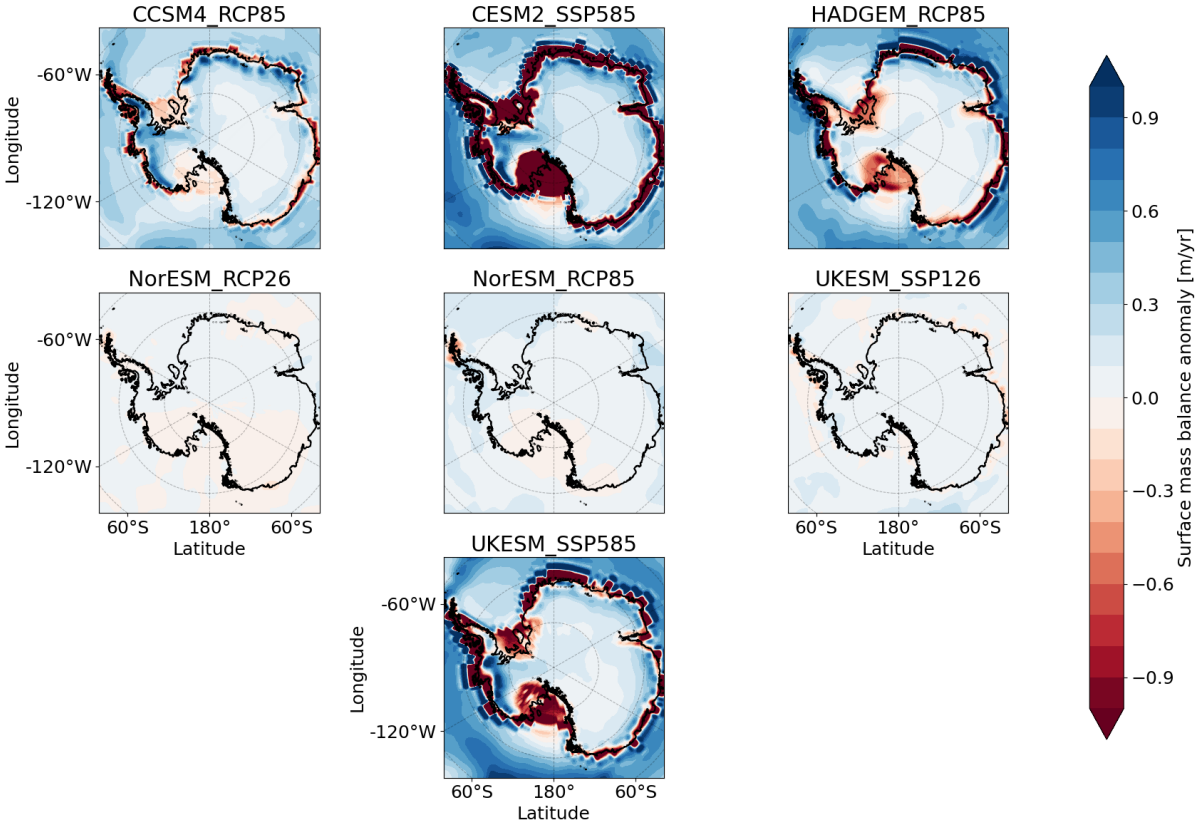

Figure S11. Surface mass balance (SMB) anomalies simulated by the five ESMs. The average of the years 2280-2300 is shown. The observed grounding line position is shown in black.

Table S1. Variables used in this study.

Variables	Units	Definition
b	m	Bedrock height above sea level
$bmlt$	m yr^{-1}	Basal melt rates under floating ice
C_c	-	Coulomb C
C_r	-	Basal friction relaxation target
H	m	Modelled ice thickness
H_{obs}	m	Observed ice thickness
N	Pa	Effective pressure
TF_{base}	K	Thermal forcing applied at the ice shelf draft
u	m yr^{-1}	Ice velocity in the x-direction
v	m yr^{-1}	Ice velocity in the y-direction
u_b	m yr^{-1}	Basal velocities magnitude
$u_{x,b}$	m yr^{-1}	Basal velocity in the x-direction
$u_{y,b}$	m yr^{-1}	Basal velocity in the y-direction
δT	K	Ocean temperature correction
s	m	Surface elevation
β	Pa yr m^{-1}	Basal traction parameter
η	Pa yr	Effective viscosity
τ_b	Pa	Basal shear stress

Table S2. Parameters and their units and values used in this study.

Parameters	Values	Units	Definition
c_{pw}	3974	J kg^{-1} K^{-1}	Specific heat of seawater
g	9.81	m s^{-2}	Gravitational acceleration
H_0	100	m	Ice thickness inversion scale factor
L_f	3.34 * 10^5	J kg^{-1}	Latent heat of fusion
m	3	-	Basal friction exponent
T_r	0	K	Relaxation target of the ocean temperature inversion
u_0	200	m yr^{-1}	Yield velocity
r	0.5	-	Strength of inversion regularization
ρ_i	917	kg m^{-3}	Density of ice
ρ_w	1027	kg m^{-3}	Density of ocean water
τ	100	yr	Time scale in the inversion
γ_0	30000	m yr^{-1}	Basal melt rate coefficient
L	4000	m	Length scale of the Gaussian term

References

Morlighem, M., Rignot, E., Binder, T., Blankenship, D., Drews, R., Eagles, G., Eisen, O., Ferraccioli, F., Forsberg, R., and Fretwell, P.: Deep glacial troughs and stabilizing ridges unveiled beneath the margins of the Antarctic ice sheet, Nature Geoscience, 13, 132-137, 2020.

Rignot, E., Mouginot, J., and Scheuchl, B.: Ice flow of the Antarctic ice sheet, Science, 333, 1427-1430, 2011.

Smith, B., Fricker, H. A., Gardner, A. S., Medley, B., Nilsson, J., Paolo, F. S., Holschuh, N., Adusumilli, S., Brunt, K., and Csatho, B.: Pervasive ice sheet mass loss reflects competing ocean and atmosphere processes, Science, 368, 1239-1242, 2020.

Zwally, H. J., Li, J., Robbins, J. W., Saba, J. L., Yi, D., and Brenner, A. C.: Mass gains of the Antarctic ice sheet exceed losses, Journal of Glaciology, 61, 1019-1036, 2015.